September 25th - 28th, 2017
INTERFACES
architecture . engineering . science IASS 2017 hamburg

Proceedings of the IASS Annual Symposium 2017
"Interfaces: architecture . engineering . science"
September 25 - 28th, 2017, Hamburg, Germany
Annette Bögle, Manfred Grohmann (eds.)

Geometric Optimization of a Reciprocal Floor-Framing System with Self-Weight and Area-Loading Considerations

Gerry IP*, Corentin FIVET[a]

*Massachusetts Institute of Technology, ip.gerry@gmail.com
[a] Swiss Federal Institute of Technology (EPFL), Structural Xploration Lab, corentin.fivet@epfl.ch

Abstract

This paper explores the geometric optimization of a planar reciprocal frame (RF) floor framing structure, focusing on the triangular topology. The structural performance of the frames is computed and plotted against the geometric parameters for various load cases. The load cases modelled include both symmetric and asymmetric loading on a hypothetical surface supported by the frame, and the loads are distributed to the members based on tributary areas. The two key geometric parameters studied are the rotation angle of the members at the unit RF level which defines the geometry, and the total number of members in the grid which defines the grid density. The structural performance is deduced from the total strain energy in the grid.

Results show that smaller rotation angles at the unit RF level produce more structurally efficient RF grids. Depending on the grid density and load case, the optimal angle lies between 4 and 8.2 degrees. To some extents, these values mean that optimum geometries for RF under area-loading considerations tend to reduce lever-arms to a minimum. It is also found that the optimal angle remains relatively unchanged for a given grid density between the symmetric and asymmetric load cases.

Keywords: Reciprocal Frame, Structural Optimization

1. Introduction

Reciprocal frame (RF) structures consist of linear members that support one another within a closed circuit, hence the origin of the term "reciprocal". This mutually supporting nature of the structure enables spans that are much greater than the length of an individual member, thus resolving the problem of satisfying long spans with shorter members (Kohlhammer & Kotnik, [4]; Popovic Larsen, [6]; Pugnale & Sassone, [7]).

Reciprocal frames are often sloped, as the stacking of members on top of each other naturally creates a gradient. The offset distance between the centerline of two connected members is referred as the eccentricity; however, flat RF structures with zero eccentricity can be achieved through notching. Flat RF grids primarily transfer loads in bending, while in eccentric configurations, loads are transferred through both axial and bending. Built examples of RF structures commonly employ timber, as it is an inexpensive material that is easy to work with during construction due to its smaller size, is easily notched, and has generally good behavior in bending (Popovic Larsen, [6]).

2. Problem Statement

Given that RF structures can come in a wide variety of topologies, geometries, and forms, what constitutes an "optimal" RF structure is not well understood yet. Since the embodied carbon of a structure comprises 50% of its total carbon footprint during its lifetime (Kaethner & Burridge, [3]), there is environmental and economic value in differentiating an efficient RF structure from non-efficient ones. With a motivation to benefit the practical application of RF grids as a floor or roof framing structure, the goal of this research is to generate results that will serve as useful rules of thumb for designers who are examining the use of a planar RF grid in their structure. Therefore, the question is how geometry

impacts the structural efficiency of an RF structure, and whether there is a particular geometry that is optimal across both symmetric and asymmetric load cases.

This paper focusses on a planar RF grid with a triangular topology, which consists of 3 members at the unit RF level. The geometry of an RF grid is defined by two variables; the rotation angle of the members, which dictates the size of the engagement window; and the density of the grid, which dictates the number of members comprising the grid. The engagement window refers to the triangle at the unit RF level. The three smallest possible grid densities are explored: the first with 12 members in total, or 6 unit RFs; the second with 42 members (24 unit RFs), and the third with 156 members (96 unit RFs). In this paper, the grid densities are referred to by the number of unit RFs they consist of.

3. Literature Review

Despite being a structural system that has been around for centuries, RF structures have not been commonly adopted in practice. Researchers suggest that it is likely because their structural behavior was never well understood. Structural systems are often selected for a given design problem on the basis of appropriateness given the loading conditions, span requirements, and architectural goals. As Parigi & Kirkegaard [5] note, it is unclear under what circumstances would a reciprocal frame be a good fit as a structural system.

Gelez, Aubry & Vaudeville [2] studied planar RF grids with the rectangular topology, where they proposed two mathematical formulas pertaining to the structural analysis of a given RF grid: one that provides the value of maximum bending moment, and another that provides the value of bending moment and deflection at any location. They also compared the structural behavior of the RF grid to an equivalent flat grid, and found that the RF grid was not competitive with respect to bending moments and deflections. However, the distribution of bending moments was more even in the RF grid, and when subjected to an irregular perimeter geometry, the RF grid performed better in terms of distributing the support reactions (Figure 1).

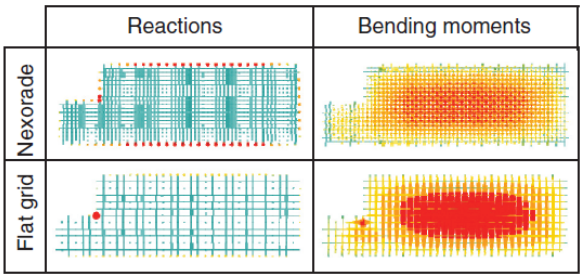

Figure 1. Comparison between an RF grid and a regular grid for an irregular perimeter [4].

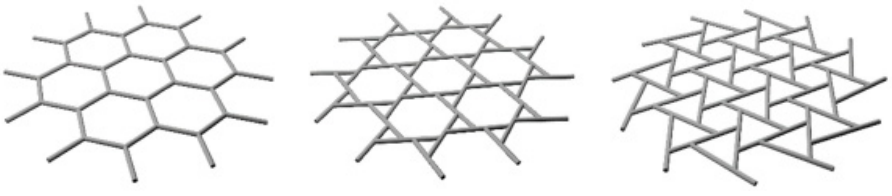

Figure 2. Examples of RF grid configurations studied by Parigi and Kirkegaard [5].

Parigi & Kirkegaard [5] studied the structural efficiency of various 2D and 3D RF configurations with the triangular topology. They explored the effect of geometric parameters on structural performance of 8 different RF geometries, with varying eccentricities of the members. The structural efficiency of each

was taken as the value of maximum stress and displacement, and the two load cases consisted of a uniform line load on each member (symmetric), or a uniform line load on half of each member (asymmetric).

Although this research paper is similar in principle to the research performed by Parigi & Kirkegaard [5], it differs by addressing some of the points for future work that were outlined in their paper and including new ones. The first difference is the use of global values such as total strain energy in assessing the structural performance, as opposed to the local values of maximum stress and displacement. Using global values would better capture the efficiency of the structure as a whole, because it would account for the contributions each member has in the performance of the grid. The second difference is the consideration of pin connections as opposed to fixed between elements, which reflects the likelihood of rotational freedom between members in reality. A third difference in the methodology is the modelling of the loads. In this paper, loads are distributed onto the members by tributary area, which reflects possible loading scenarios for a hypothetical structural floor framing system. This contrasts with previous work, where members received identical uniform loads or point loads.

4. Methodology

This section will briefly outline the methodology used to generate the parameterized structural analysis model of the planar RF structure with triangular topology. The procedure is summarized in Figure 3. Custom python scripts have been created inside Grasshopper, a graphical editor for Rhino, a 3-D modelling software [9]. Structural analysis is performed using the Karamba plugin for Grasshopper [8]. Hand calculations were also done to check the Karamba analysis outputs.

Three grid densities are studied: N = 6, N = 24, N = 96. Following the sequence described on Figure 3, sub-section 4.1 explains how the grid is generated, sub-section 4.2 describes are how self-weight and external loads are computed, and sub-section 4.3 details the structural analysis and the objective function for the optimization. The sequence is then iterated until an optimum is found.

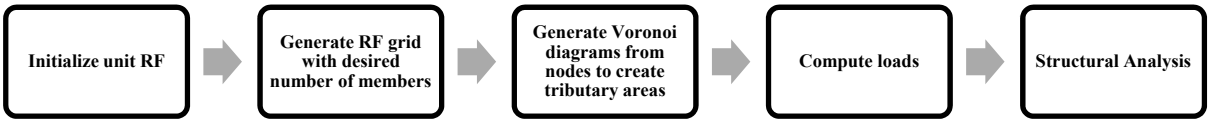

Figure 3. Sequence used to generate parameterized model.

4.1. Grid generation

Generation of the parameterized structural model begins with creating the unit RF (Figure 4). The unit RF with triangular topology is initialized from an equilateral triangle, with each member rotated about a vertex. This rotation angle is the key variable that distinguishes different geometries. It ranges from 0 to 30 degrees in 0.1 degree increments. The resulting triangle that is enclosed by the three members has side lengths referred to as the engagement length. In this paper, we are interested in the ratio of the engagement length divided by the member length. After the unit RF is defined, larger grids are generated through a series of polar arrays. Examples of the N = 24 grid at different rotation angles is shown in Figure 5.

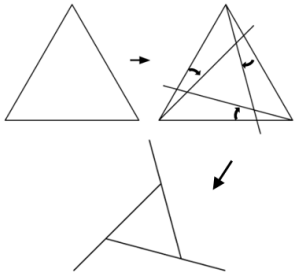

Figure 4. Generating the unit RF. The overhanging portions are trimmed after rotating the members.

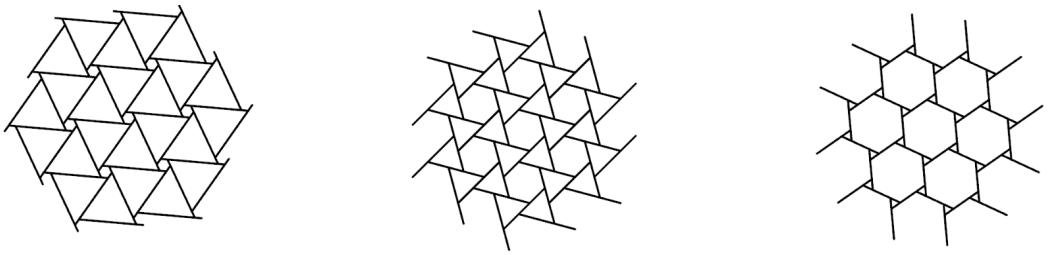

Angle: 5°
Engagement Ratio: 0.82

Angle: 15°
Engagement Ratio: 0.67

Angle: 25°
Engagement Ratio: 0.42

Figure 5. Examples of the N = 24 grid at various rotation angles.

4.2. Area-Loading and Self-Weight

The loads to each member are distributed by tributary area over the full polygon circumscribing the grid. Since the width tributary to each member varies along its length, this non-uniform distributed load is approximated by a series of discrete point loads (Figure 6). The tributary areas are generated through Voronoi diagrams.

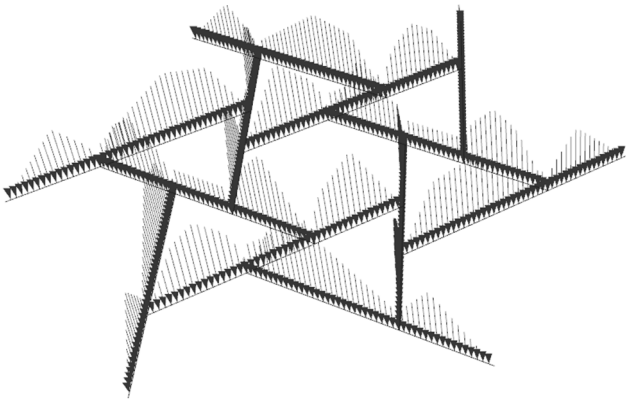

Figure 6. Discretized distributed loads, calculated based on tributary areas.

Self-weight is applied as a uniform line load, and all the members are assumed to be solid wood. The member cross-section varies for each grid density, as the members are sized according to the maximum moment of all load cases at any rotation angle (*i.e.* only one cross-section is used for each grid density). Maintaining a constant cross-section across all rotation angles is beneficial as the optimal geometry would only be defined by geometry and not also the self-weight. Furthermore, it was determined that the member self-weight contributed minimally to the bending demand of the members, which meant that the lack of cross-section optimization at each rotation angle would not skew the results.

For the two denser grids, the bending moments begin to increase exponentially for rotation angles beyond 27 degrees, so the value of moment used for sizing is capped off at that point. This is to avoid grossly oversizing the members.

Two symmetrical and two asymmetrical load cases are modelled in the analysis, which are represented in Figure 7. The loads are based on service level values for the expected occupancy, which is assumed to be a floor framing structure supporting an assembly area. Therefore, the surface load and concentrated load are 4.8 kPa and 8.9 kN respectively [1].

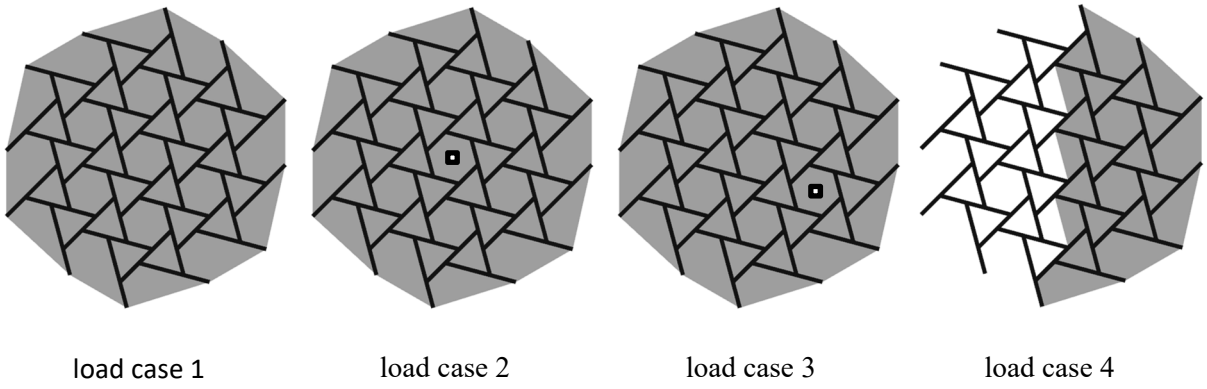

Figure 7. Schematic of applied loads. The shaded area indicates the extent of area load; the square point indicates the location of concentrated load.

4.3. Structural Analysis & Optimization

The final step is to analyze the parameterized structural model, using finite element analysis implemented by the Karamba plugin for Grasshopper [8]. The joints at the member connections are modelled as pins, as it would be difficult to achieve full fixity of the connection in reality. The boundary support conditions are rollers, with one pin for lateral resistance. Lateral loads and torsion are neglected, and only linear elastic behavior is assumed in the analysis.

A hand calculation to verify the analysis results generated by the Karamba plugin was performed, and resulted in values within 10% of the software output. Therefore, the results output by Karamba can be accepted with confidence.

The objective function for the optimization is defined by the following expression, where $M_i(x)$ is the bending moment distribution of the length L of element i, $M_{i,max}$ is the maximum bending moment occurring in element i, E is the modulus of elasticity, and I is the moment of inertia for the strong axis. Both E and I are assumed constant over the length of the members and for each member. The length L is the same for all the members.

$$min\left(\sum_i \int_L \frac{M_i(x)^2}{2EI(x)}dx\right) \approx min\left(\sum_i \frac{M_{i,max}^2 L}{2EI}\right) = min\left(\sum_i M_{i,max}^2\right)$$

The resulting value (right expression) is similar to the total strain energy due to the bending moments (left expression) except that bending moments are here assumed constant and maximum over the full length of each element i. This formulation simplifies the computation and is more in line with the fact that the elements will have a constant section size (and consequently a constant volume) determined by the maximum bending moment it will have to withstand, for a given grid density. The final expression

(right) is independent of the material and the cross-section. It only depends on the geometry of the system and the loading. It will be referred to as Strain Energy Factor in the following sections.

5. Results

The general trend across all grid densities and load cases is that the more structurally efficient grids are those with a smaller rotation angle, and therefore larger engagement ratio. A common pattern is that the Strain Energy Factor initially decreases to a minimum at a rotation angle between 4 and 9 degrees, then increases for rotation angles beyond. Recall that a lower value for the Strain Energy Factor corresponds to a greater efficiency. The exact value of rotation angle at which the optimal structural performance exists varies between the different grid densities and load cases. An interesting observation is the flattening of the structural performance curves at a rotation angle of about 20 degrees for both the N = 6 and N = 96 grids; this is in contrast with the N = 24 grid.

It is important to note that the results from the structural analysis are based on several assumptions. Buckling out of plane due to bending, and the effect of stress concentrations at the joints due to the assumed notching of members are not considered. Since certain rotation angles have joints that are closer together, the stress concentrations at these areas could have an effect on the efficiency of the structure that is not captured in the strain energy.

5.1. N=6 Grid results

For the N = 6 grid, the optimal geometry occurs at a rotation angle of 8.2 degrees for load cases 1-3 and 6.4 degrees for load case 4. The Strain Energy Factor for each rotation angle is plotted in Figure 8. The geometries at the optimal angles are shown in Figure 9.

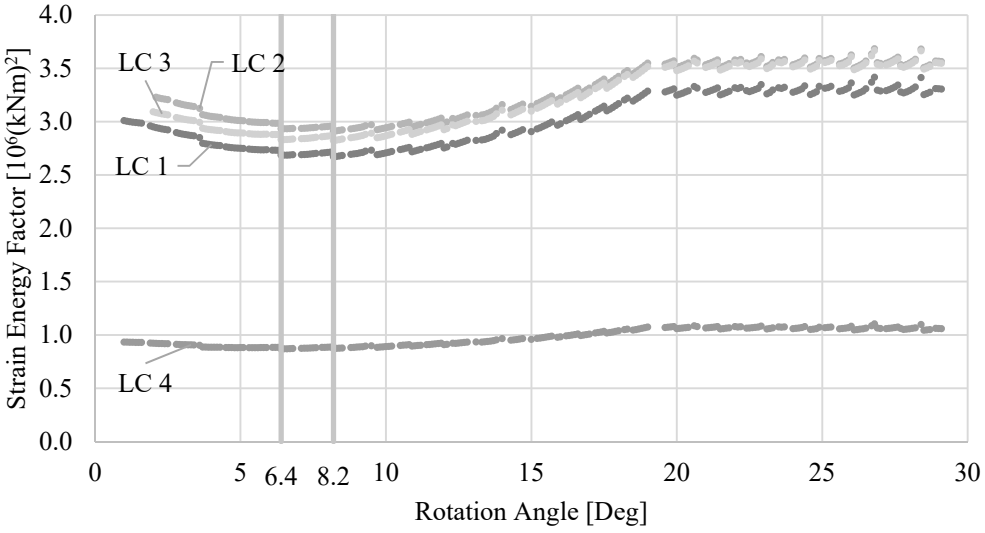

Figure 8. Structural performance vs. rotation angle of all load cases for the N=6 grid.

Rotation Angle: 8.2°
Engagement Ratio: 0.82

Rotation Angle: 6.4°
Engagement Ratio: 0.86

Figure 9. Optimal geometries for the N=6 grid.

5.2. N = 24 Grid Results

For the N = 24 grid, the optimal geometry occurs between 4.2 and 4.0 degrees. The Strain Energy Factor for each rotation angle is plotted in Figure 10. The geometries at the bounding optimal angles are shown in Figure 11.

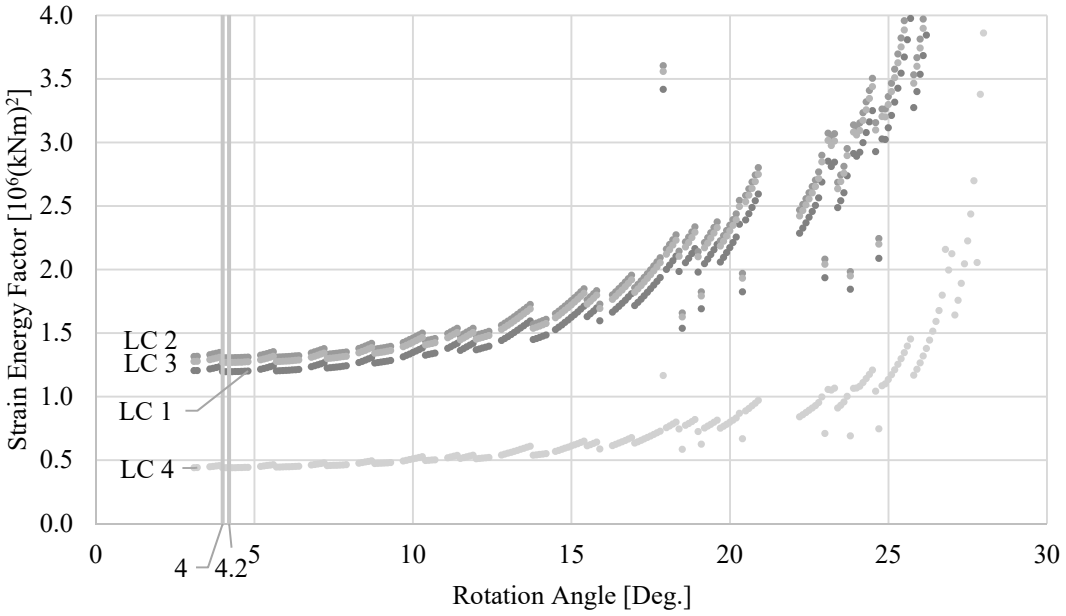

Figure 10. Structural performance vs. rotation angle of all load cases for the N=24 grid.

Rotation Angle: 4.2°
Engagement Ratio: 0.92

Rotation Angle: 4.0°
Engagement Ratio: 0.93

Figure 11. Optimal geometries for the N=24 grid.

5.3. N = 96 Grid Results

Similar to the two previous grid densities, the optimal rotation angle does not occur at an extremity but at 4.1 degrees, and in this case is the optimal for all load cases. In addition, the angle is very similar to that of the N = 24 optimal (4.2 degrees). The Strain Energy Factor for each rotation angle is plotted in Figure 12. The geometries at the optimal angles are shown in Figure 13.

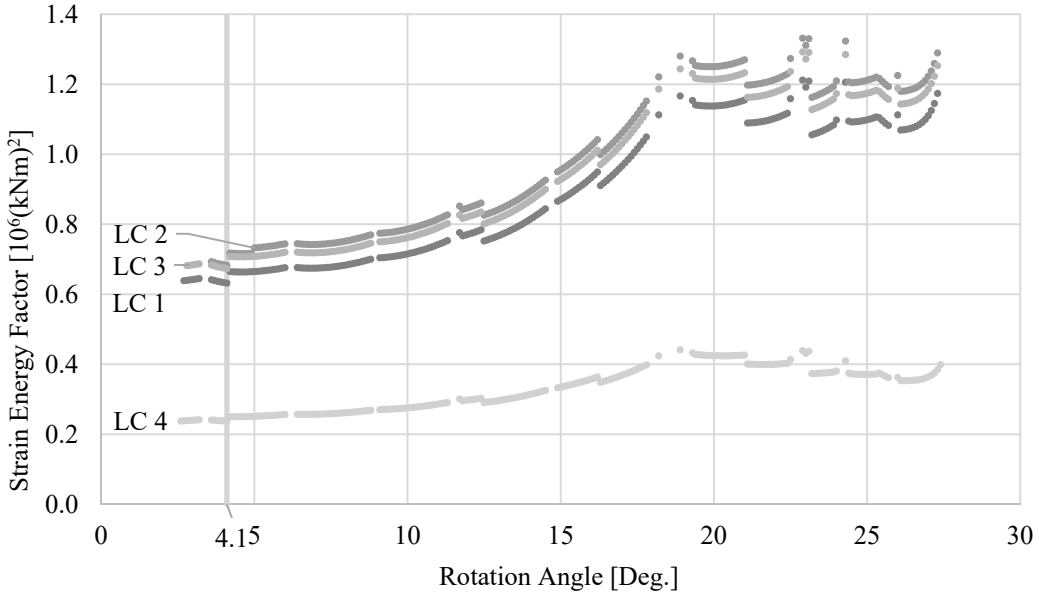

Figure 12. Structural performance vs. rotation angle of all load cases for the N = 96 grid.

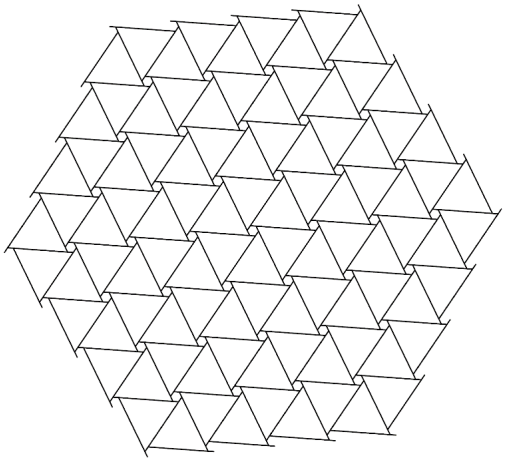

Rotation Angle: 4.1°
Engagement Ratio: 0.91

Figure 13. Optimal geometry for the N = 96 grid.

6. Conclusion

This research complements the small body of work that has been done in investigating the structural efficiency of reciprocal frame (RF) structures. In contrast with past investigations on the structural behavior of RF grids where all members receive identical uniform loading, this research adds an additional level of refinement through the inclusion of non-uniform loading as a result of the tributary distribution of a floor load. Furthermore, the metric of structural performance is derived from the global strain energy, which better captures the efficiency of a reciprocal frame as a whole.

The results are promising as they suggest that planar RF structures are a good fit for cases where asymmetric loading may occur frequently, since their geometric configuration would not be much less efficient than if it was loaded symmetrically. Given that asymmetric loading often occurs for a floor or roof framing structure, the results suggest that a planar RF structure is a good fit for that application.

Potential for future work includes expanding the research to additional RF topologies, such as the rectangular topology. Since geometries with the rectangular topology cannot be described in terms of a rotation angle, the size of the engagement window is suggested to be the parameterized variable. It would be valuable to determine whether structural performance would similarly decrease as the engagement window becomes smaller, and whether the most efficient geometry is the same for both symmetric and asymmetric loading.

References

[1] American Society of Civil Engineers. *Minimum Design Loads for Buildings and Other Structures*. ASCE 7-10, 2013.

[2] Gelez S., Aubry S., and Vaudeville B., Behavior of a Simple Nexorade or Reciprocal Frame System, *International Journal of Space Structures*, vol. 26, no. 4, 2011, pp. 331-342.

[3] Kaethner S.C. and Burridge J.A., Embodied CO2 of structural frames, *The Structural Engineer*, vol. 90, no. 5, 2012, pp. 33-40.

[4] Kohlhammer T. & Kotnik T. *Systemic Behaviour of Plane Reciprocal Frame Structures.* Structural Engineering International, vol.21, num. 1, 2011, pp. 80-86.

[5] Parigi D. and Kirkegaard P.H., Structural Behaviour of Reciprocal Structures, in *International Association for Shell and Spatial Structures (IASS) Symposium*, Poland, 2013.

[6] Popovic Larsen O., Reciprocal Frame (RF) Structures: Real and Exploratory, *Nexus Network Journal,* Article vol. 16, no. 1, Apr 2014, pp. 119-134.

[7] Pugnale A. & Sassone M., Structural Reciprocity: Critical Overview and Promising Research/Design Issues, *Nexus Network Journal,* Article vol. 16, no. 1, Apr 2014, pp. 9-35.

[8] Preisinger C., *Karamba*, 1.1.0 ed, 2016.

[9] Robert McNeel & Associates, *Grasshopper*, 0.9.0076 ed: Robert McNeel & Associates, 2016.